Method to Estimate Human Inattention in Teleoperation of Mobile Robots

Franco Penizzotto * **Emanuel Slawiñski** * **Vicente Mut** *

* *Instituto de Automática, Universidad Nacional de San Juan, San Juan, Argentina (e-mail: fpenizzotto, slawinski, vmut@inaut.unsj.edu.ar).*

Abstract: In teleoperation of mobile robots the operator is remotely located. As a result, generally the human perception of the remote environment is distorted affecting the mission negatively. Visual information can be degraded because of video images bandwith, time lags, frame rates, point of view and motion effects among other reasons. Although many researchers have proposed a variety of methods for measuring perception, just a few can be used in control closed loop systems. This paper aims to provide a novel metric to the human visual inattention upon risk for a remotely navigated mobile robot. We present both qualitative and quantitative guidelines for designing the metric in a teleoperation of a mobile robot. The method allows to incorporate the metric in a control closed loop system, and task consists in guiding the robot from an initial point to a final one as quick as possible, considering the constraint of avoiding collisions. Furthermore, a haptic cue based on the metric is proposed in order to help the human to avoid collisions. A system stability analysis considering time varying delays is proposed. Additionally, we present a human in the loop experiment of a teleoperation of a 3D mobile robot simulator in order to remark the advantages of using human factors in the controller.

Keywords: Selective of attention, Visual Attention, Human Factors, Teleoperation of mobile robots, Metric.

1. INTRODUCTION

Robot teleoperation allows the execution of different tasks in remote environments including possibly dangerous and harmful jobs for the human operator (Sheridan, 1992a). In the teleoperation systems of robots with force feedback, a user completes some task and physically interacts with the environment through a master-slave system. Thus, several control schemes and strategies for the teleoperation of mobile robots have been developed in order to solve tasks such as land surveying in inaccessible or remote sites, transportation and storage of hazardous material, inspection of high-voltage power lines, de-activation of explosive devices, high-risk fire control, pesticide and fertilizer crop spraying and dusting, mining exploration and various other tasks (Sheridan, 1992b; Sayers, 1999; Slutski, 1998; Fiorini and Oboe, 1997; Elhajj et al., 2003; Lam et al., 2009; Sanders, 2010).

Recent years have seen an increasing development in the bilateral teleoperation algorithms, like (Daly and Wang, 2014) and (Willaert et al., 2014), but (Fong and Thorpe, 2001) states that despite the advances in automation, will always exist the need of a human in the loop for the teleoperation of vehicles. Some researchers have focused his attention over the consideration of human operator aspects, due to the overall performance of bilateral teleoperation systems relies on them. (Chen et al., 2007) presents an examination of more than 150 papers covering human performance issues and mitigation solutions for teleoperated systems.

In the case of guiding a remote mobile robot, visual feedback can often be limited by the on-board camera restriction, like restricted field of view (FOV) and poor resolution (McCarley and Wickens, 2005; Diolaiti and Melchiorri, 2002). If the operator perception is reduced due to a poor visual stimulus, the teleoperation could result in undesired collisions with remote obstacles. Providing haptic cues could mitigate this limitations.

(Ratwani et al., 2010) stated that Perception is one of the human factors elements most used to develop on-line measures. There are several reasons why perception is probably the most relevant of the three stages, since the perception stage is the first to occur (as it is shown in Endsley, 1995); without perception, neither comprehension nor projection can take place. In addition, (Jones and Endsley, 1996) has empirically shown that lack of perception is responsible for over 75 % of pilot errors.

1.1 Previous works

Although (Son et al., 2013) achieve useful human centered design and evaluation about haptic cueing to help the operator in a teleoperation of multiple robots, neither

⋆ This work was supported by the Consejo Nacional de Investigaciones Científicas y Técnicas (CONICET), the National University of San Juan and the Automatic Institute of the National University of San Juan.

the control or the interface are adapted to the human performance.

Recently, a number of researchers have focused their attention on human perspective studies in mobile robot teleoperation, but few works have addressed the case of including metrics of command execution in the control loop. This means that the control law is designed for an on-line adaptation to the human performance, which can be very varies during a task and between different operators. On-line control adaptation requires on-line measures, and these kind of metrics are difficult to design. Typically measures use subjective methods (Taylor, 1990), query based methods such as (Endsley, 1995) and (Durso and Dattel, 2004), and implicit performance methods (Andre et al., 1991). While these methods are suitable for understanding some aspects of human performance, facilitating cognitive engineering design, and improving training, they are not suitable for closed control loops. In (Salmon et al., 2006), there is a summary of Situation Awareness measurement techniques. Only *Process Indices* or some *Real Time* methods can be used as control feedback signal, like Eye tracker (based on human gaze), Verbal Protocol Analysis (based on human verbalization) and the Situation Present Assessment Method (SPAM) (Durso et al., 1998). Generally, the on-line visual tracker methods are based on counting how many times users look an specific place.

On the other hand, (Slawiński et al., 2012) proposed a teleoperation control framework where a mobile robot is guided using a haptic device, which allows the operator to perceives information of the remote site. (Penizzotto et al., 2014) proposes an on-line metric about commands performance in the teleoperation of a mobile robot without time delay, which was considerer in the control law. (Chavez et al., 2010) present a method to modelling the inattention of a human while driving a car, based on the human gaze and the forward path. They have demonstrate that in the system presented, the human inattention was similar to a variable delay.

1.2 Objective and Outline

The aim of this work is to propose an on-line method to get the human visual inattention upon risk in teleoperation of mobile robots, and include this metric in the control system considering a dynamic environment. The method proposed quantifies the human visual inattention, including the decision of where he decides to focus his gaze and some cognitive processes related to the visual information processing. The method is non-intrusive and it does not require to freeze the task or any kind of query. The metric obtained can be incorporated in a control closed loop, modifying the Human Machine Interface, and/or the controller parameters. In this case, we have proposed a haptic cue based on force feedback, which depends on the metric proposed. We show the stability analysis proposed for the system, and we demonstrate that the inclusion of this haptic cue strengths the stability of the errors of interest. A human in the loop experiment was performed when an operator drives a remote simulated robot navigating over a 3D virtual reality simulator environment.

This work is organized as follows: First, the frame work of the system is presented. After that, section 3 exposes the

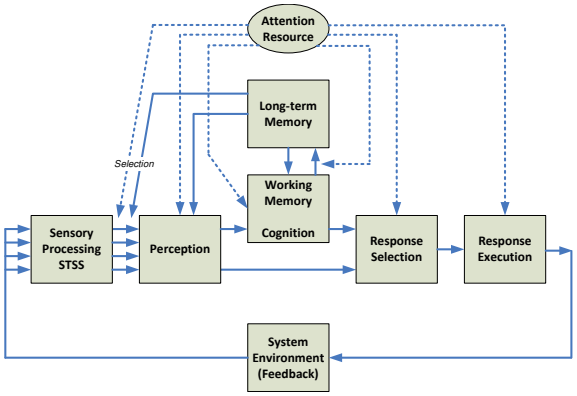

Fig. 1. A model of human information processing stages (Wickens and Hollands, 2000)

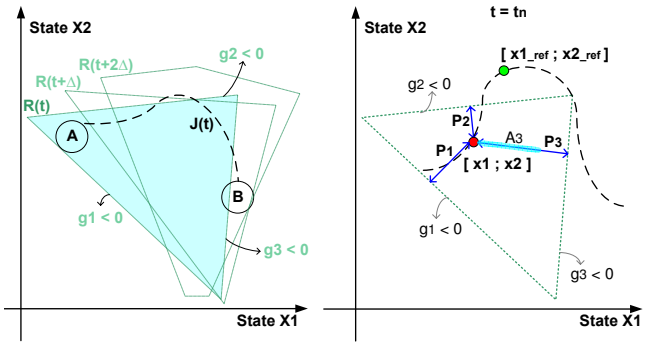

Fig. 2. Definition of the Problem

teleoperation control system with the haptic cue including the metric. In the section 4 we define the metric and expose the main method proposed. Next, on section 6 an explanation about the implementation of the system and some experiments are shown. Finally, the conclusions are given.

2. FRAMEWORK

In order to understand how humans process input information, figure 1 shows a model of the human information processing stages presented in (Wickens and Hollands, 2000), who described each stage.

On the other hand, a Human-Robot operated system is characterized by a human operator interacting with a remote working environment through the robot. Multiple tasks are treated. Some of them are managed by the automation systems and others by the user. The *Environment* is formed by the place where the robot is situated, mobile and stuck obstacles and other robots operated by other humans or controllers.

These systems can be represented by a *robot state vector* X, one or more *goals* to be tracked (references vector) $J(t)$, and variable *constraints* to accomplish $R(t)$.

Figure 2(a) represents a two states system, with a variable restriction zone to the states. The main task to be achieved by the operator consists in guiding the state vectors $X = [x_1(t) \ \dots \ x_n(t)]$ (in this work it corresponds to the position of the robot), from the initial point A (X_0) to the final one B (X_f), as nearby as possible to the trajectory $J = [x_{1_{ref}}(t) \ \dots \ x_{n_{ref}}(t)]$ (n is the num-

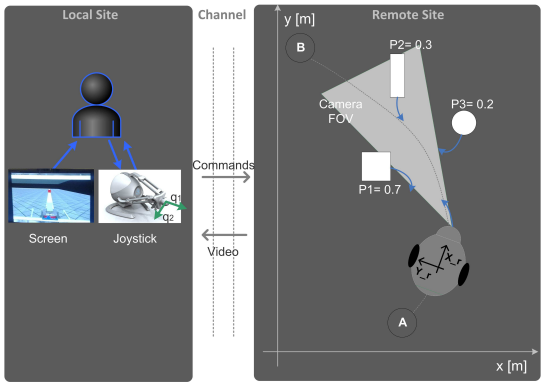

Fig. 3. Static human-robot interaction

ber of state variables of the robot). At the same time, the state vector X should remains as far as possible from the boundaries of the Variant Constraints Region $R = [g_1(X, t, Environment) \ \ldots \ g_p(X, t, Environment)]$. This means that the robot should follow a reference trajectory but avoiding positions included in the constrains.

In figure 2(b) it is shown a representation of the human-robot system face in this work. The main task consists in guiding the remote robot from current values $X = [x_1 \ ; \ x_2]$ to reference values $X_{ref} = [x_{1_{ref}} \ ; \ x_{2_{ref}}]$. In this teleoperation systems we want to avoid collisions with others robots or obstacles, so a restriction for the robot position arises. From the gap between $X(t)$ (robot position) and each limitation $g_i(x, Environment, t)$ (position of obstacles) emerges a level of risk (named $P = [P_1 \ P_2, P_p]$) due to each i restriction (obstacle). A value of 1 means that the constraint is being violated (collapse state) and 0 means that there is no way to reach the limits g_i. The operator should guide the robot keeping each elements of $P \in [0, 1]$ as low as possible.

Due to the current field of view of the camera and the gaze over the screen, the operator can poorly perceive the risk, which is represented by $A(t)$, defined in this work as the level of attention over the risk $P(t)$. It is assumed that $P(t)$ changes dynamically. Additionally, the quantity of obstacles or elements that generates a risk situation is priori unknown and variable in time. Secondary tasks can appear although they were not modeled by the designer of the control system. The operator must decide the level of priority that the secondary task represents against attending each source of danger P_i (i identifies each obstacle).

Figure 3 shows a general situation faced in this work, where a user want to drive the robot from A to B (main task) without crashing against any obstacle. Besides, visual feedback is limited by the on-board camera restrictions (triangle of the figure), like limited field of view (FOV) and poor resolution.

3. BILATERAL TELEOPERATION

3.1 Control Architecture on the Remote Site

This paper proposes a teleoperation systems in which a human operator drives a wheeled robot in an unknown environment, while he perceives the environment near the robot through visual feedback. In addition, a haptic force feedback in the master helps the human in the guidance of the robot. Figure 4 shows the block representation of the system proposed.

On the master side, a haptic device using two-degree-of-freedom (DOF) were considered ($n = 2$), which is modelled by

$$M_m(q) \ \ddot{q}_m + C(q_m, \dot{q}_m) \ \dot{q_m} + g(q_m) = \tau_m + f_h \qquad (1)$$

where $q_m(t) \in \Re^{nx1}$ is the joint position of the master (in this work $q_m(t) = [q_{m_1}(t) \ \ q_{m_2}(t)]^T$, $n = 2$); $\dot{q_m}(t) \in \Re^{nx1}$ is the joint velocity (in this work $\dot{q_m}(t) = [\dot{q}_1(t) \ \ \dot{q_m}_2(t)]^T$) ; $M_m(q_m) \in \Re^{nxn}$ is the inertia matrix; $C(q_m, \dot{q_m}) \in \Re^{nxn}$ is the matrix representing centripetal and Coriolis torques; $g(q_m) \in \Re^{nx1}$ is the gravitational torque; $f_h \in \Re^{nx1}$ is the torque caused by the human operator force, and $\tau_m \in \Re^{nx1}$ is the control torque applied to the master.

For the case of teleoperation of wheeled robots, the dynamic model of a unicycle-type mobile robot is considered [15]. It has two independently actuated rear wheels and is represented by,

$$D\dot{\eta} + Q(\eta)\eta = \tau_s + f_e \qquad (2)$$

where $\eta = [\eta_1 \ \ \eta_2]^T$ is the robot velocity vector with η_1 and η_2 representing the linear and angular velocity of the mobile robot, f_e is the force caused by the elements of the environment on the robot, $D = [m \ 0 \ ; \ 0 \ i]$ and $Q = [0 \ - ma\omega \ ; \ ma\omega \ 0]$; where m is the mass of the robot, i is the rotational inertia, and a is the distance between the mass centre and the geometric centre. In addition, $\tau = [u_1 \ \ u_2]$ involves a control force $u_1 = \frac{1}{r_\omega}(u_{left} + u_{right})$ and a control torque $u_2 = \frac{1}{r_\omega}(u_{right} - u_{left})$, where $r_\omega > 0$ is the radius of the wheels, $c > 0$ is the half-width of the cart, and u_{left} and u_{right} are the torques of the left and right rear wheels respectively. Furthermore, the communication channel adds a forward time delay h_1 and a backward time delay h_2. Generally, these delays are time-varying and different between them (asymmetric delays).

Figure 5 shows the teleoperated system of this work, whose control structure is well known in teleoperation systems of manipulator robots (Nuño et al., 2008; Hua and Liu, 2010), but in this case, a metric of a human aspect is incorporated in the control loop of the haptic device.

The control scheme in the remote side establishes the control actions to the robot, as follows,

$$\tau_s = k_s(k_g q_m(t - h_1) - u_k(t) - \eta(t)) + Q(\eta)\eta(t) \qquad (3)$$

where $\tau_s \in \Re^{2x1}$ is the torque applied to the robot and $k_g \in \Re^{2x1}$ converts position of the master to a velocity command (compatible with the restrictions about maximum velocity of the mobile robot). The parameter $k_s \in \Re^{2x1}$ is a positive constant and represents a proportional gain. The delayed command of the operator can be written as $u_h = k_g q_m(t - h_1)$. u_k is a velocity impedance (bounded) that reduces the intensity of the commands on the remote site in order to prevent collisions ((Slawiski et al., 2012)).

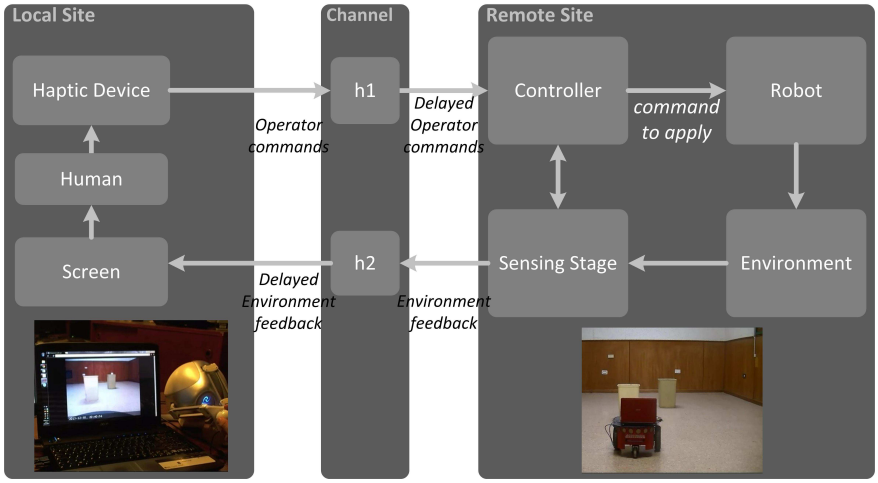

Fig. 4. Haptic bilateral teleoperation system

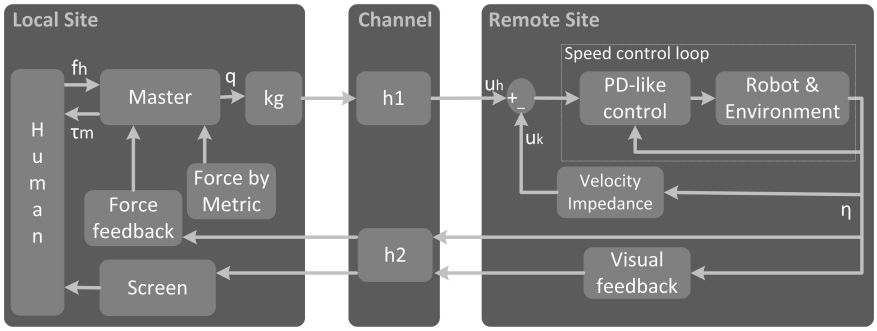

Fig. 5. Control applied to the mobile robot and haptic feedback

3.2 Control Architecture in Local Site. Haptic feedback

In the literature, two classes of haptic cues are typically considered as force feedback sources in conventional teleoperation systems: 1) The mismatch between the command of the master and the execution of the slave in terms of position or velocity, which is called as master-slave tracking error ($q - x_s$ or $\dot{q} - \dot{x_s}$); 2) the force measured by a force sensor mounted on the slave in contact with the environment f_s; 3) a linear combination of both, (Hashtrudi-Zaad and Salcudean, 2001). Generally, a PD control control law is applied to the first error mentioned while a P control is suitable for the second error.

In our case, some consideration should be noted. First, the master-slave tracking error defined upon cannot be directly applied given that the desired velocity for the robot is proportional to q rather than $\dot{q}$ in accordance with our control scheme. Second, we do not want real contact force acting on the slave side since avoiding obstacles is desired in this task. So, there is not a real f_s. Finally, the metric proposed about wrong visual selection of attention allow us to include this information as a haptic cue to the human, in order to reduce the mobility of the robot. Hence, we define our force feedback control as

$$\tau_m = -k_m(t)\ q_m(t) - \alpha_m\ \dot{q}_m(t) + g(t) \tag{4}$$

where $\tau_m \in \Re^{2x1}$ is the torque applied to the master, $\alpha_m \in \Re^{2x2}$ (diagonal) is a constant damping gain that is tuned in order to assure the stability of the system (better explained in section 5), $k_m(t) = k_{m0} + \Delta k_m\ (t, q_m\dot{q}_m, Me) > \varepsilon$ ($k_m(t) \in \Re^{2x2}$, diagonal) represents the scaling of force applied to the master, where

$$\Delta k_m(t) = Me(t)(\varepsilon + k_{m0}) \tanh\left(\frac{q_m\dot{q}_m}{(q_m\dot{q}_m)_{max}}\right) \tag{5}$$

is a variable gain proportional to the metric to human visual inattention ($Me(t)$), which rises the total elasticity of the master when the operator is having a bad selection of visual attention (this metric is defined in section 4). In addition, $g(t)$ is a torque that compensate the gravitational force of the master. $\varepsilon > 0$ is a tuning parameter for scaling Me. It can be noted that k_m is bounded and $\Delta k_m\ q_m\ \dot{q}_m \geq 0$.

If the system senses a poor performance of the human attention in front of risk situations (risk of collision with obstacles), the elasticity rises and the joystick tends to the origin (the operator needs more effort to move the joystick). This cue helps the user to prevent a bad command due to bad attention.

4. METRIC

For a teleoperated system of a mobile robot, we stablish a metric called *Visual Selective Inattention* (Me), defined as:

"The inattention that a human operator has about the existing risk in the remote site, only based on his visual

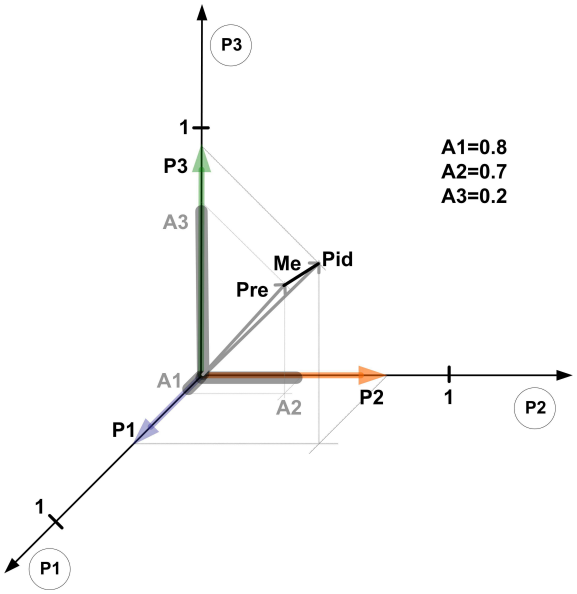

Fig. 6. Quantitative components of the metric proposed

selection of attention" (in this work the level of risk is considered as the robot-obstacle collisions probability).

4.1 Qualitative definitions

- Ideal Visual Perception ($P_{id}(t)$):
  Human perfect perception of the risk around the remote site. P_{id} is the human exact knowledge of the actual robot-obstacle collisions probabilities.

$$P_{id}(t) = [P_1(t),\ P_2(t),\ \ldots\ ,\ P_p(t)] \tag{6}$$

- Possible Visual Perception ($P_{re}(t)$):
  Maximum human perception of the risk around the remote site, based only on his visual information. P_{re} is the human visual estimation of the actual robot-obstacle collisions probabilities.

$$P_{re}(t) = (P_1(t)A_1(t),\ P_2(t)A_2(t),\ \ldots\ ,\ P_p(t)A_p(t)) \tag{7}$$

  Where A_i represents the maximum level of the operator perception over the risk P_i, only based on his visual information. A_i estimates how accurate the operator can estimate P_i based on his visual inspection ($0:1$ normalized). Modelling A_i is presented in section 4.2.

Considering (6) and (7), Me is defined as the *distance* between *Ideal Visual Perception* and *Possible Visual Perception*, establishing a quantitative measurement of the human visual disattention about the surrounding risk.

$$Me(t) = \|P_{id}(t) - P_{re}(t)\| = \sqrt{(P_1 - P_1A_1)^2 + \ldots + (P_q - P_qA_q)^2} \tag{8}$$

$Me = 0$ means that the operator is able to achieve an excellent perception of the risk around, and $Me = \sqrt{q}$ means that there is no way to perceives the collision probabilities due to the q obstacles.

In figure 6, a graphic representation for the metric is presented (3 obstacles). Te robot has a collision probability against each obstacle (P_i), but he is not able to estimate each risk with the same accuracy (A_i). Visual inattention (Me) corresponds to the distance between the ideal *knowledge of the collision probabilities* and the maximum possible estimation of them.

This method allows a direct comparison of the inattention of one moment t_1 with s objects against other t_2 with w objects. The upper limit of the scale is non linear and is higher when appears more obstacles.

4.2 Calculation of the factor A_i

It is well known that, although selective attention can occur without a change in direction of gaze (Egeth and Yantis, 1997), our gaze is often driven by our need to attend. We can also assume that when the visual information about a risk situation is not available at the initial cognitive stage, the situation can be perceived. It is reasonable to think that a bad selection of the visual attention will lead to poor perception. As it was mentioned before, we are interested in the detecting poor perception of collision probabilities. We want to know how accurate can the collisions probability be estimated by the human. It is difficult to estimate the level of good perception, but we can deduce about bad perception after knowing that if the information of the visual stimulus (risk) is not available, probably bad perception is achieve.

This paper complements the user's gaze with two cognitive visual process about selective of attention in order to get a better measure of poor visual perception. First, only a small region of the visual field perceives details. This region is called *fovea* and it is about 2 degrees of visual angle. Outside this region, the visual details start to degrade. Second, we consider the characteristic of a human to retain the signals perceived by his sensory processing system (STSS) for an interval of time, in which he could still recover visual information. The time of the STSS depends on each person, therefore, we have considered the average time (Wickens and Hollands, 2000). This work uses three stages to get the final variable $A(t)$.

Figure 7 represents the field of view of the operator (triangle), respect to the Reference Frame sited on board the robot. The user inspects the remote environment through visual scanning on the screen (local site) in order to estimate the collisions probabilities, but his visual information is limited. φ_{visual} is the angle of the fixation point of the human's field of view respect to the reference frame (screen). This angle is measured with a gaze tracker software. φ_{object} is the angle of the obstacle respect to the robot frame., and it is measured estimating the position of the obstacle respect to the robot (measured with a laser scanner) and the camera rotation angle. φ_{fovea} is the angle of the object respect to the middle of the field of view (Visual fixation point).

Taking into account the scope of the human visual channel d_{visual} and φ_{fovea}, we can determine if the obstacle is in or out of the human field of view (FOV). Equation (9) shows the values to A_{in} when the obstacle is IN or OUT of the FOV.

$$A_{in} = \left\{ \begin{array}{ll} 1, & IN \\ 0, & OUT \end{array} \right\} \quad (9)$$

From the figure 10, it can be noted that $\varphi_{fovea} = \varphi_{object} - \varphi_{visual}$. The left subplot of figure 8 shows A_{fovea} factor as a function of φ_{fovea}. The central zone is the one called fovea region. For simplicity, we have considered that the visual fixation point locates a Gauss function in order to achieve an approximated model for the degradation of the information when going away the foveal region. This function weighs the visual information contained in the screen (position of an obstacle) when appears an obstacle around the fixation point, and it is described by equation 10. Angle φ_{wide} depends on the spacial distribution and complexity of the information. Fovea region is bounded to 20° for this application, empirically determined after trial and error. Therefore, $\varphi_{wide} = 40$.

$$A_{fovea} = e^{-\frac{\varphi^2_{fovea}}{2(\varphi_{wide})}} \quad (10)$$

On the right subplot, it is show the function for modelling the Short-Term Sensory Store (STSS) described above. After the disappearance of a visual stimulus, during a time T_{STSS} (time interval considered for the visual STSS), the information of the stimulus can be recover from the STSS by the cognition human stage. Particularly for the human visual channel (VSTM: Visual Short Term Memory), 0.50 seconds or more are considered, depending on the information involved (Luck and Hollingworth, 2008).

Finally, figure 9 shows the accomplishment of the visual features mentioned. First, for each obstacle, the A_{in} factor considers the relative position between the obstacles and the gaze user. Then, A_{fovea} is calculated as it was previously described. After that, the $STSS$ stage takes the signal $A_{in}A_{fovea}$ as the input signal and distinguishes between increasing and decreasing slopes. When rising slopes occur, the output signal A_i copies the value of the input signal. This means that the object is moving to the center of the field of view (fixation point). On the contrary, when ascents slopes take place (object moving away of the visual fixation point), the output A_i adds a transport delay T_{STSS} in the input signal. This action is done until a new increasing slope is detected.

4.3 Quantitative definitions

Figure 10 shows several situations that throw different values of the metric proposed. In the case named 1, the metric takes the best value ($Me = 0$) since the human can have a good visual attention respect to both obstacles ($A_1 = A_2 = 1$). When the operator can attends only to the obstacle 1, the metric achieves 0.20 (case 2). Case 3 is comparable with case 2 since the risk levels are equal, but differs in the limitation of visual attention over the obstacle 1 ($A_i = 0.50$), causing $Me = 0.44$. It is high because the information is not present in the cognition stage. In the next case (4), risk due to obstacle 2 can be attended by the user, while a high risk caused by the obstacle 1 is can not be perceived by the operator ($Me = 0.80$) due to a poor selection of visual attention. Case (5) has the worst attention condition since the user does not see any obstacle during a time interval greater than T_{STSS} ($Me = 0.82$)

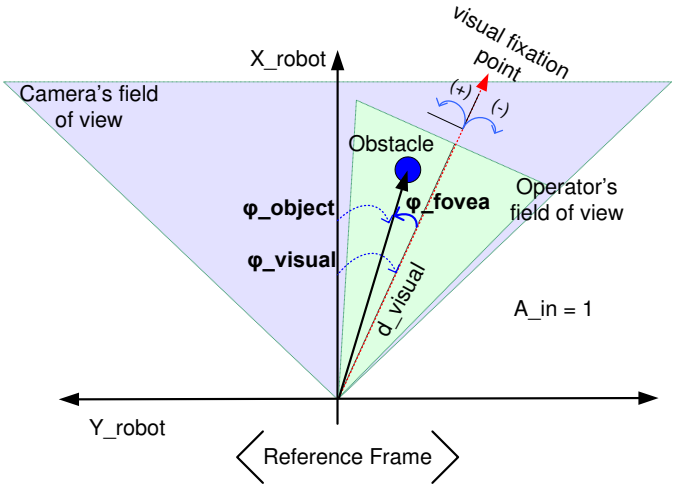

Fig. 7. Visual operator reference axis and field of view

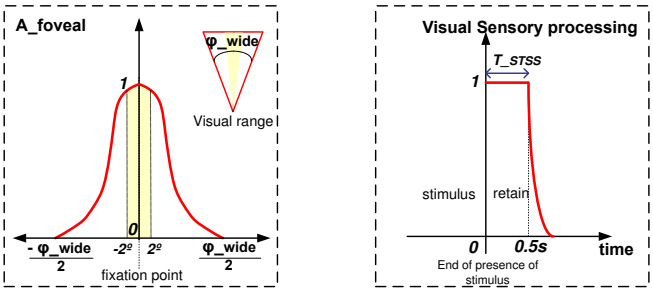

Fig. 8. Functions of A_{fovea} and Visual Sensory Processing

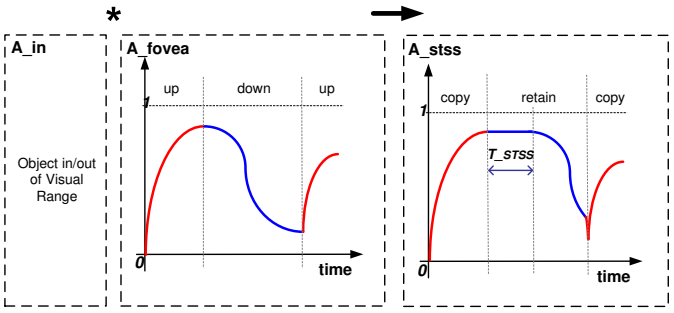

Fig. 9. Stages to reach A_i

and ($Me = 1.40$). Finally in (6), being $t(n) - t(n-2) < 0.5$, with 0.5 as the retain period of time for the visual STSS, visual information (localization) of both obstacles is still available for the cognitive process, therefore, $A_1 = A_2 = 1$ and $Me = 0$.

It is important to remark the difference between this method and the well known gaze tracker. Taking into account the case 6, for simply computing the visual attention based only on the user's gaze at the actual time $t(n)$, we would conclude that it is not possible to attend the risk around ($A_1 = A_2 = 0$) as the operator is not looking at the obstacle. On the other hand, using the method proposed, the inattention of the operator is low because he could extract information about the pending conflict ($A_1 = A_2 = 1$).

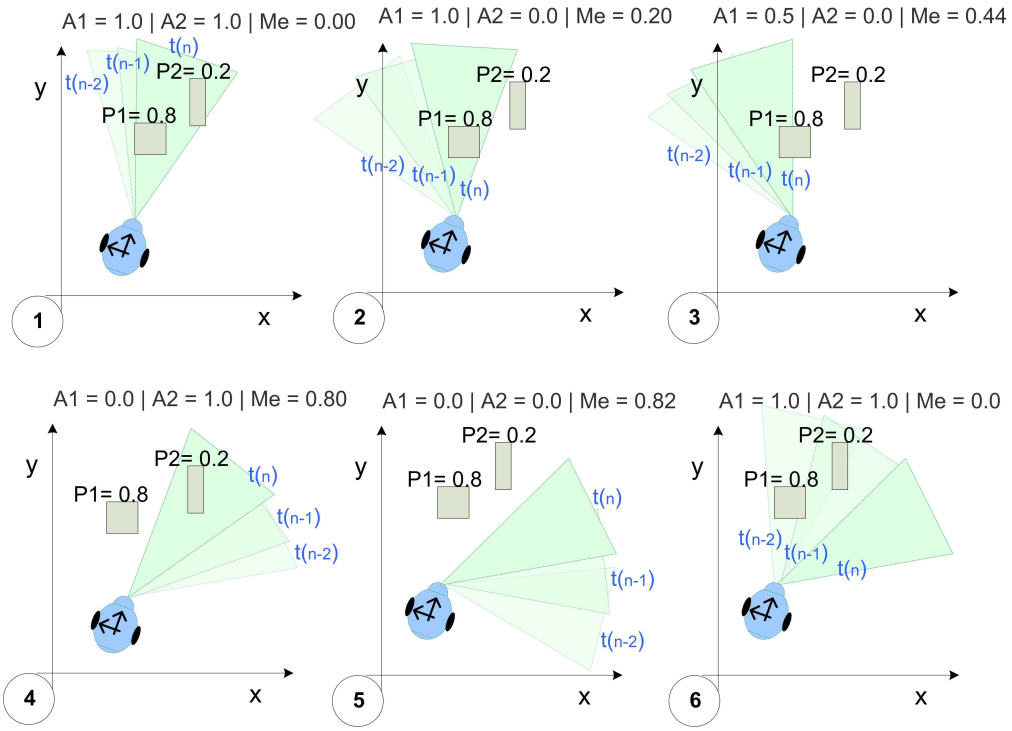

Fig. 10. Dissimilar situation for the metric proposed

5. SYSTEM STABILITY ANALYSIS

It is important to highlight the common states variables that should be analyzed in a teleoperation system. They are: 1) the master-slave tracking error, 2) the dimension of the master velocity ($\dot{q}$ should be bounded or tend to 0) and 3) the dimension of the acceleration of the master ($\ddot{q}$ should tend to 0).

Before to deepen about de stability analysis, the following ordinary properties, assumptions and lemmas will be used in it:

On the other hand, the following ordinary properties, assumptions and lemmas will be used in this paper:

Property 1: The inertia matrices $\mathbf{M_m}(\mathbf{q_m})$ and $\mathbf{D}$ are symmetric positive definite.

Property 2: The matrix $\dot{\mathbf{M}}_\mathbf{m}(\mathbf{q_m}) - 2\mathbf{C_m}(\mathbf{q_m}, \dot{\mathbf{q}}_\mathbf{m})$ is skew-symmetric.

Property 3: There exists a $k_c > 0$ such that $\mathbf{C_m}(\mathbf{q_m}, \dot{\mathbf{q}}_\mathbf{m})\,\dot{\mathbf{q}}_\mathbf{m} \leq k_c|\dot{\mathbf{q}}_\mathbf{m}|$.

Assumption 1: The time delays $h_1(t)$ and $h_2(t)$ are bounded. Therefore, there exist positive scalars $\bar{h}_1$ and $\bar{h}_2$ such that $0 \leq h_1(t) \leq \bar{h}_1$ and $0 \leq h_2(t) \leq \bar{h}_2$ for all t.

Assumption 2: The human operator behaves in a non-passive way, represented by the following model,

$$\mathbf{f_h} = -k_h\mathbf{q_m} - \alpha_h\dot{\mathbf{q}}_\mathbf{m} + \mathbf{f_a} \tag{11}$$

where k_h and α_h are positive intrinsic parameters of the human operator, and $\mathbf{f_a}$ is the active component of $\mathbf{f_h}$. It is assumed that $\mathbf{f_a} \in L_2$.

Assumption 3: The environment force and the non-passive component of the human force are bounded, this is $|\mathbf{f_e}| \leq \bar{f}_e$ and $|\mathbf{f_a}| \leq \bar{f}_a$ where $\bar{f}_e$ and $\bar{f}_a$ are positive values.

Lemma 1 (Hua and Liu, 2010)**:** For real vector functions $\mathbf{a}(.)$ and $\mathbf{b}(.)$ and a time-varying scalar $h(t)$ with $0 \leq h(t) \leq \bar{h}$, the following inequality holds

$$-2\mathbf{a}^{\mathrm{T}}(t)\int_{t-h(t)}^{t}\mathbf{b}(\xi)d\xi - \int_{t-h(t)}^{t}\mathbf{b}^{\mathrm{T}}(\xi)\mathbf{X}\mathbf{b}(\xi)\,d\xi \leq h(t)\,\mathbf{a}^{\mathrm{T}}(t)\,\mathbf{X}^{-1}\mathbf{a}(t) \leq \bar{h}\mathbf{a}^{\mathrm{T}}(t)\,\mathbf{X}^{-1}\mathbf{a}(t) \tag{12}$$

where $\mathbf{X} > 0$ is a positive definite matrix.

Next, a positive definite functional $V_i = V_1+V_2+V_3+V_4 > 0$ is proposed. It is important to remark that there is not an equilibrium point but a Krasovskii-like equilibrium solution that depends on the state $\mathbf{x} := [\dot{\mathbf{q}}_\mathbf{m} \quad (\boldsymbol{\eta} - k_g\mathbf{q_m}) \quad \mathbf{q_m}]$ in the time interval $[(t - h_1 - h_2)\ ,\ t]$ (Niculescu, 2001; Slawiñski et al., 2006).

The functional is formed by five parts: V_1 represents the motion energy of the master and mobile robot, V_2 represents the potential energy of the error between the master and the mobile robot, V_3 represents the potential energy of the master, and V_4 is included for mathematical reasons in order to transform the terms that include delayed variables to terms with non-delayed variables. The first three sub-functional are proposed in the following manner:

$$V_1 = \frac{1}{2}\dot{\mathbf{q}}_\mathbf{m}^{\mathrm{T}}\mathbf{M_m}(\mathbf{q_m})\,\dot{\mathbf{q}}_\mathbf{m} \tag{13}$$

$$V_2 = \frac{1}{2}(\boldsymbol{\eta} - k_g\mathbf{q_m})^{\mathrm{T}}(\boldsymbol{\eta} - k_g\mathbf{q_m}) \tag{14}$$

$$V_3 = \frac{1}{2}(k_h + k_{m0})\,\mathbf{q}_\mathbf{m}^{\mathrm{T}}\mathbf{q_m} \tag{15}$$

The time derivative of V_1 along the master dynamics (1), taking into account properties 1 and 2, is the following one,

$$\begin{aligned}\dot{V}_1 &= \frac{1}{2}\,\dot{\mathbf{q}}_\mathbf{m}^{\mathrm{T}}\dot{\mathbf{M}}_\mathbf{m}\dot{\mathbf{q}}_\mathbf{m} + \dot{\mathbf{q}}_\mathbf{m}^{\mathrm{T}}\mathbf{M}_\mathbf{m}\ddot{\mathbf{q}}_\mathbf{m} \\ &= \frac{1}{2}\,\dot{\mathbf{q}}_\mathbf{m}^{\mathrm{T}}\dot{\mathbf{M}}_\mathbf{m}\dot{\mathbf{q}}_\mathbf{m} \\ &\quad + \dot{\mathbf{q}}_\mathbf{m}^{\mathrm{T}}\mathbf{M}_\mathbf{m}\mathbf{M}_\mathbf{m}^{-1}\left(\boldsymbol{\tau}_\mathbf{m} + \mathbf{f}_\mathbf{h} - \mathbf{C}_\mathbf{m}\dot{\mathbf{q}}_\mathbf{m} - \mathbf{g}_\mathbf{m}\right) \\ &= \dot{\mathbf{q}}_\mathbf{m}^{\mathrm{T}}\left(\boldsymbol{\tau}_\mathbf{m} + \mathbf{f}_\mathbf{h} - \mathbf{g}_\mathbf{m}\right) \\ &= \dot{\mathbf{q}}_\mathbf{m}^{\mathrm{T}}\left(\boldsymbol{\tau}_\mathbf{m} - \mathbf{g}_\mathbf{m}\right) + \dot{\mathbf{q}}_\mathbf{m}^{\mathrm{T}}\mathbf{f}_\mathbf{h} \end{aligned} \tag{16}$$

Now, if the control action $\boldsymbol{\tau}_\mathbf{m}$ (4) is included in (16), and considering (11), it yields,

$$\begin{aligned}\dot{V}_1 = &-\dot{\mathbf{q}}_\mathbf{m}^{\mathrm{T}}\,k_{m0}\,\mathbf{q}_\mathbf{m} - \dot{\mathbf{q}}_\mathbf{m}^{\mathrm{T}}\,\boldsymbol{\Delta}\mathbf{k}_\mathbf{m}\,\mathbf{q}_\mathbf{m} \\ &- \dot{\mathbf{q}}_\mathbf{m}^{\mathrm{T}}\left(\alpha_m + \alpha_h\right)\dot{\mathbf{q}}_\mathbf{m} + \dot{\mathbf{q}}_\mathbf{m}^{\mathrm{T}}\mathbf{f}_\mathbf{a} - k_h\,\dot{\mathbf{q}}_\mathbf{m}^{\mathrm{T}}\mathbf{q}_\mathbf{m}\end{aligned} \tag{17}$$

Next, $\dot{V}_2$ along the dynamics of the wheeled robot (2) is obtained as,

$$\begin{aligned}\dot{V}_2 &= \left(\boldsymbol{\eta} - k_g\mathbf{q}_\mathbf{m}\right)^{\mathrm{T}}\left(\dot{\boldsymbol{\eta}} - k_g\dot{\mathbf{q}}_\mathbf{m}\right) \\ &= \left(\boldsymbol{\eta} - k_g\mathbf{q}_\mathbf{m}\right)^{\mathrm{T}}\dot{\boldsymbol{\eta}} - k_g\left(\boldsymbol{\eta} - k_g\mathbf{q}_\mathbf{m}\right)^{\mathrm{T}}\dot{\mathbf{q}}_\mathbf{m} \qquad (18) \\ &= k_s\left(\boldsymbol{\eta} - k_g\mathbf{q}_\mathbf{m}\right)^{\mathrm{T}}\mathbf{D}^{-1}(k_g\mathbf{q}_\mathbf{m}\left(t - h_1\right) - u_k - \boldsymbol{\eta} \\ &\quad + k_g\mathbf{q}_\mathbf{m} - k_g\mathbf{q}_\mathbf{m}) - k_g\left(\boldsymbol{\eta} - k_g\mathbf{q}_\mathbf{m}\right)^{\mathrm{T}}\dot{\mathbf{q}}_\mathbf{m} \\ &\quad + \left(\boldsymbol{\eta} - k_g\mathbf{q}_\mathbf{m}\right)^{\mathrm{T}}\mathbf{D}^{-1}\mathbf{f}_\mathbf{e} \qquad (19) \\ &= -k_s\left(\boldsymbol{\eta} - k_g\mathbf{q}_\mathbf{m}\right)^{\mathrm{T}}\mathbf{D}^{-1}\left(\boldsymbol{\eta} - k_g\mathbf{q}_\mathbf{m}\right) \\ &\quad - k_g\left(\boldsymbol{\eta} - k_g\mathbf{q}_\mathbf{m}\right)^{\mathrm{T}}\dot{\mathbf{q}}_\mathbf{m} + \left(\boldsymbol{\eta} - k_g\mathbf{q}_\mathbf{m}\right)^{\mathrm{T}}\mathbf{D}^{-1}\mathbf{f}_\mathbf{e} \\ &\quad - k_sk_g\left(\boldsymbol{\eta} - k_g\mathbf{q}_\mathbf{m}\right)^{\mathrm{T}}\mathbf{D}^{-1}\int_{t-h_1}^{t}\dot{\mathbf{q}}_\mathbf{m}\left(\xi\right)d\xi \\ &\quad -k_s\left(\boldsymbol{\eta} - k_g\mathbf{q}_\mathbf{m}\right)^{\mathrm{T}}\mathbf{D}^{-1}u_k \qquad (20)\end{aligned}$$

Additionally, the time derivative of V_3 is calculated,

$$\dot{V}_3 = \left(k_h + k_{m0}\right)\mathbf{q}_\mathbf{m}^{\mathrm{T}}\dot{\mathbf{q}}_\mathbf{m} \tag{21}$$

It is possible to appreciate in (20) there is delayed variable that makes the stability analysis difficult,(the term: $-k_sk_g\left(\eta - k_gq_m\right)^T D^{-1}\int_{t-h_1}^{t} q_m\left(\xi\right)d\xi$. For solving this, V_5 is proposed as follows:

$$V_4 = \int_{-\bar{h}_1}^{0}\int_{t+\theta}^{t}\dot{\mathbf{q}}_\mathbf{m}^{\mathrm{T}}\left(\xi\right)\mathbf{X}\dot{\mathbf{q}}_\mathbf{m}\left(\xi\right)d\xi\;d\theta \tag{22}$$

where $\mathbf{X}$ is a positive definite matrix.

From (22), and considering assumption 1, $\dot{V}_4$ can be computed by,

$$\dot{V}_4 \leq +\,\bar{h}_1\dot{\mathbf{q}}_\mathbf{m}^{\mathrm{T}}\,\mathbf{X}\,\dot{\mathbf{q}}_\mathbf{m} - \int_{t-h_1}^{t}\dot{\mathbf{q}}_\mathbf{m}^{\mathrm{T}}\left(\xi\right)\,\mathbf{X}\,\dot{\mathbf{q}}_\mathbf{m}\left(\xi\right)d\xi \tag{23}$$

$\dot{V}$ can be written considering equations (17)-(23) in the following way:

$$\begin{aligned}\dot{V} &= \dot{V}_1 + \dot{V}_2 + \dot{V}_3 + \dot{V}_4 \\ &= -\dot{\mathbf{q}}_\mathbf{m}^{\mathrm{T}}\,k_{m0}\,\mathbf{q}_\mathbf{m} - \dot{\mathbf{q}}_\mathbf{m}^{\mathrm{T}}\,\boldsymbol{\Delta}\mathbf{k}_\mathbf{m}\,\mathbf{q}_\mathbf{m} \\ &\quad - \dot{\mathbf{q}}_\mathbf{m}^{\mathrm{T}}\left(\alpha_m + \alpha_h\right)\dot{\mathbf{q}}_\mathbf{m} + \dot{\mathbf{q}}_\mathbf{m}^{\mathrm{T}}\mathbf{f}_\mathbf{a} - k_h\,\dot{\mathbf{q}}_\mathbf{m}^{\mathrm{T}}\mathbf{q}_\mathbf{m} \\ &\quad -k_s\left(\boldsymbol{\eta} - k_g\mathbf{q}_\mathbf{m}\right)^{\mathrm{T}}\mathbf{D}^{-1}\left(\boldsymbol{\eta} - k_g\mathbf{q}_\mathbf{m}\right) \\ &\quad - k_g\left(\boldsymbol{\eta} - k_g\mathbf{q}_\mathbf{m}\right)^{\mathrm{T}}\dot{\mathbf{q}}_\mathbf{m} + \left(\boldsymbol{\eta} - k_g\mathbf{q}_\mathbf{m}\right)^{\mathrm{T}}\mathbf{D}^{-1}\mathbf{f}_\mathbf{e} \\ &\quad - k_sk_g\left(\boldsymbol{\eta} - k_g\mathbf{q}_\mathbf{m}\right)^{\mathrm{T}}\mathbf{D}^{-1}\int_{t-h_1}^{t}\dot{\mathbf{q}}_\mathbf{m}\left(\xi\right)d\xi \\ &\quad -k_s\left(\boldsymbol{\eta} - k_g\mathbf{q}_\mathbf{m}\right)^{\mathrm{T}}\mathbf{D}^{-1}u_k \\ &\quad + \left(k_h + k_{m0}\right)\mathbf{q}_\mathbf{m}^{\mathrm{T}}\dot{\mathbf{q}}_\mathbf{m} \\ &\quad + \bar{h}_1\dot{\mathbf{q}}_\mathbf{m}^{\mathrm{T}}\,\mathbf{X}\,\dot{\mathbf{q}}_\mathbf{m} - \int_{t-h_1}^{t}\dot{\mathbf{q}}_\mathbf{m}^{\mathrm{T}}\left(\xi\right)\,\mathbf{X}\,\dot{\mathbf{q}}_\mathbf{m}\left(\xi\right)d\xi\end{aligned} \tag{24}$$

On one hand, the three terms that include $\dot{\mathbf{q}}_\mathbf{m}^\mathbf{T}\mathbf{q}_\mathbf{m}$ can be cancel between them. On the other hand, using the property $-2ab \leq a^2 + b^2$, we can state that

$$-k_g\left(\boldsymbol{\eta} - k_g\mathbf{q}_\mathbf{m}\right)^{\mathrm{T}}\dot{\mathbf{q}}_\mathbf{m} \leq \frac{k_g^2}{4}\dot{\mathbf{q}}_\mathbf{m}^\mathbf{T}\,\dot{\mathbf{q}}_\mathbf{m} + \left(\boldsymbol{\eta} - k_g\mathbf{q}_\mathbf{m}\right)^{\mathrm{T}}\left(\boldsymbol{\eta} - k_g\mathbf{q}_\mathbf{m}\right) \tag{25}$$

Next, the two terms with integrals can be conveniently joined using Lemma 1 (12) as it is shown in Eq. (26)

$$\begin{aligned}&-\int_{t-h_1}^{t}\dot{\mathbf{q}}_\mathbf{m}^{\mathrm{T}}\left(\xi\right)\mathbf{X}\dot{\mathbf{q}}_\mathbf{m}\left(\xi\right)d\xi \\ &\quad - k_sk_g\left(\boldsymbol{\eta} - \mathbf{q}_\mathbf{m}\right)^{\mathrm{T}}\mathbf{D}^{-1}\int_{t-h_1}^{t}\dot{\mathbf{q}}_\mathbf{m}\left(\xi\right)d\xi \\ &\quad \leq \frac{1}{4}\bar{h}_1k_g^2k_s^2\left(\boldsymbol{\eta} - \mathbf{q}_\mathbf{m}\right)^{\mathrm{T}}\mathbf{D}^{-1}\mathbf{X}^{-\mathbf{1}}\mathbf{D}^{-1}\left(\boldsymbol{\eta} - \mathbf{q}_\mathbf{m}\right)\end{aligned} \tag{26}$$

Then, from (24), (25) and (26), $\dot{V}$ is written as follows:

$$\begin{aligned}\dot{V} = &-\dot{\mathbf{q}}_\mathbf{m}^{\mathrm{T}}\,\boldsymbol{\Delta}\mathbf{k}_\mathbf{m}\,\mathbf{q}_\mathbf{m} - \dot{\mathbf{q}}_\mathbf{m}^{\mathrm{T}}\left(\alpha_m + \alpha_h\right)\dot{\mathbf{q}}_\mathbf{m} + \dot{\mathbf{q}}_\mathbf{m}^{\mathrm{T}}\mathbf{f}_\mathbf{a} \\ &-k_s\left(\boldsymbol{\eta} - k_g\mathbf{q}_\mathbf{m}\right)^{\mathrm{T}}\mathbf{D}^{-1}\left(\boldsymbol{\eta} - k_g\mathbf{q}_\mathbf{m}\right) \\ &+\frac{k_g^2}{4}\dot{\mathbf{q}}_\mathbf{m}^\mathbf{T}\,\dot{\mathbf{q}}_\mathbf{m} + \left(\boldsymbol{\eta} - k_g\mathbf{q}_\mathbf{m}\right)^{\mathrm{T}}\left(\boldsymbol{\eta} - k_g\mathbf{q}_\mathbf{m}\right) \\ &+\left(\boldsymbol{\eta} - k_g\mathbf{q}_\mathbf{m}\right)^{\mathrm{T}}\mathbf{D}^{-1}\mathbf{f}_\mathbf{e} - k_s\left(\boldsymbol{\eta} - k_g\mathbf{q}_\mathbf{m}\right)^{\mathrm{T}}\mathbf{D}^{-1}u_k \\ &+\bar{h}_1\dot{\mathbf{q}}_\mathbf{m}^{\mathrm{T}}\,\mathbf{X}\,\dot{\mathbf{q}}_\mathbf{m} \\ &+\frac{1}{4}\bar{h}_1k_g^2k_s^2\left(\boldsymbol{\eta} - \mathbf{q}_\mathbf{m}\right)^{\mathrm{T}}\mathbf{D}^{-1}\mathbf{X}^{-\mathbf{1}}\mathbf{D}^{-1}\left(\boldsymbol{\eta} - \mathbf{q}_\mathbf{m}\right)\end{aligned} \tag{27}$$

Regrouping terms of $\dot{V}$, we achieve to:

$$\begin{aligned}\dot{V} = &-\dot{\mathbf{q}}_\mathbf{m}^{\mathrm{T}}\,\boldsymbol{\Delta}\mathbf{k}_\mathbf{m}\,\mathbf{q}_\mathbf{m} \\ &+\dot{\mathbf{q}}_\mathbf{m}^{\mathrm{T}}\left(-\alpha_m - \alpha_h + \frac{k_g^2}{4} + \bar{h}_1\,\mathbf{X}\right)\dot{\mathbf{q}}_\mathbf{m} \\ &+\left(\boldsymbol{\eta} - k_g\mathbf{q}_\mathbf{m}\right)^{\mathrm{T}}\ldots\end{aligned}$$

$$\left(-k_s\mathbf{D}^{-1}+I+\frac{1}{4}\bar{h}_1k_g^2k_s^2\mathbf{D}^{-1}\mathbf{X}^{-1}\mathbf{D}^{-1}\right)(\boldsymbol{\eta}-k_g\mathbf{q_m})$$
$$+\dot{\mathbf{q}}_\mathbf{m}^{\mathrm{T}}\mathbf{f_a}+(\boldsymbol{\eta}-k_g\mathbf{q_m})^{\mathrm{T}}\mathbf{D}^{-1}\mathbf{f_e}$$
$$-k_s(\boldsymbol{\eta}-k_g\mathbf{q_m})^{\mathrm{T}}\mathbf{D}^{-1}u_k \quad (28)$$

Equation (28) let us conclude that: (1) considering $X^{-1}=\frac{1}{k_s^2}$, $\exists\ k_s>0$ and $\alpha_m>0$ such that $\dot{V}<0$. (2) the terms containing f_e, f_a or u_k are system disturbances bounded by other quadratic and negative term (in particular, u_k is generated by the remote controller when an obstacle is near the robot in order to avoid collisions). The three signals are bounded, so disturbances are bounded. The controller can be set to assure the stability of the system. When f_e, f_a and u_k are zero, the error will tend to zero too. Otherwise, the errors tend to a ball. In addition, the inclusion of Δk_m reinforce the stability of the errors (note that the term is always negative, except for $\dot{\mathbf{q}}_\mathbf{m}\mathbf{q_m}=\mathbf{0}$).

6. EXPERIMENTS

A Human In The Loop (HITL) experiment is proposed, defined as a model that requires human interaction. In this type of simulation a human is always part of the simulation and consequently influences the outcome in such a way that is difficult if not impossible to reproduce exactly. HITL also readily allows for the identification of problems and requirements that may not be easily identified by other means of simulation. HITL is often referred to as interactive simulation, which is a special kind of physical simulation in which physical simulations include human operators, such as in a flight simulator or a driving simulator. The experimentation consists on a teleoperation of a mobile robot running on a 3D virtual environment (developed under Simulink/Matlab) trough Internet. The communication between local and remote side was performed over a LAN network Local Network, so the time delay is almost depreciable.

Using a simulated robot allows to have a controllable environment, repeatability of the conditions of the environment and ease enforcement of experiments, which allows to have a big number of trials with different human operators or the same operator under different conditions. Although the robot is simulated, the operator, his visual feedback and the master device are real.

6.1 Participant

For this paper 10 participants (age range: 20 - 55 years) from the National University of San Juan took part in this experiments. None presented any physical disability. All of them took part in at least 3 times in each of the three cases described.

6.2 Equipment

The equipment mainly consisted on a central display (3 computer monitor 19") and a haptic device for the local side, a Local Network connection as communication channel, and a 3D simulated mobile robot with a speed control loop incorporated navigating on a virtual environment with moving obstacles around (on the remote side). The central display shows view of the camera on board the robot.

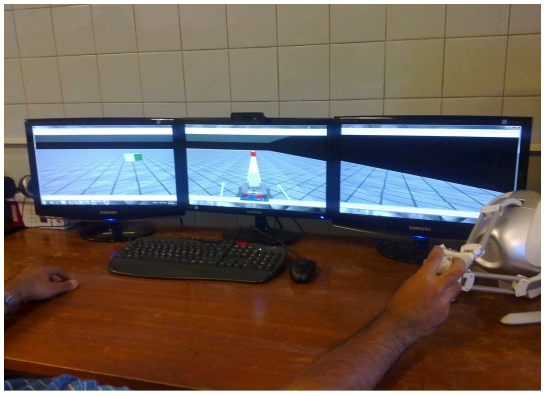

Fig. 11. Photograph to the local site of the system for the experimentations

A photograph of the local site if shown in the figure 11.

Sample time in the local side for the master device was $10ms$ due to $\dot{q}$ computation and damping force feedback ($(\alpha_m+\alpha_{VA})\dot{q}$). Data transmission rate and sample time in the remote side were made at $50ms$.

A commercial haptic device (Novint Falcon) was used as the master device. It is a three-DOF (only 2 were used) with three translational actuated axes (`http://home.novint.com/index.php/products/novintfalcon`).

In order to estimate the fixation point of the human gaze, an open-source gaze tracker developed at the IT University of Copenhagen called ITU Gaze Tracker was used (`http://www.gazegroup.org/downloads`). After an initial calibration, it estimates the coordinates $(x-y)$ of the fixation point of the gaze respect the screen, only using a webcam (in our case, `http://www.logitech.com/en-us/product/hd-pro-webcam-c920`).

Finally, instructions on manipulating the haptic device and experimental procedure were presented to the user on a pre-experiment windows information.

6.3 Control Parameters

The speed control loop on the robot is incorporated on the robot computer as a low level control loop, which is previously well adjusted, therefore, speed references send to the robot and it controller are expected to be well followed.

For the controller of the master device, we have set $k_m=diag\{10\frac{Ns}{m};\ 3\frac{Ns}{m}\}$ and $\alpha_m=diag\{2\frac{Ns}{s};\ 2\frac{Ns}{m}\}$ and $\varepsilon=20$ after a tuning procedure in which the robot was guided to an obstacle (rising the collision probability), without looking at it ($Me=1$).

Finally, in order to transform the position of the master to a speed reference, k_g is established as $k_g=diag\{20.0\frac{1}{s};\ 10.0\frac{1}{s}\}$

The range of the master positions in both axis is from $-0.05[m]$ to $0.05[m]$, therefore, the maximum speed linear and angular references are $1.0[m/s]$ and $0.5[rad/s]$.

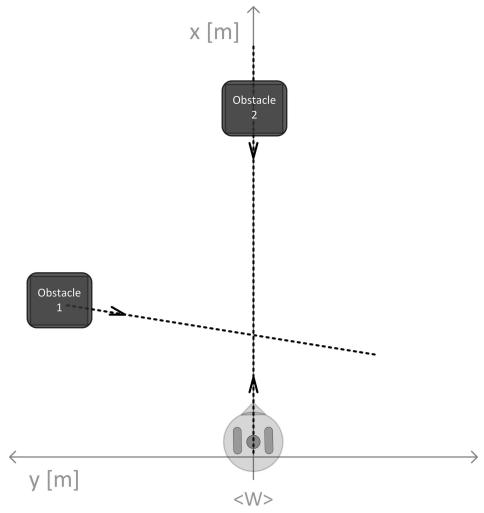

Fig. 12. Environment and path to follow

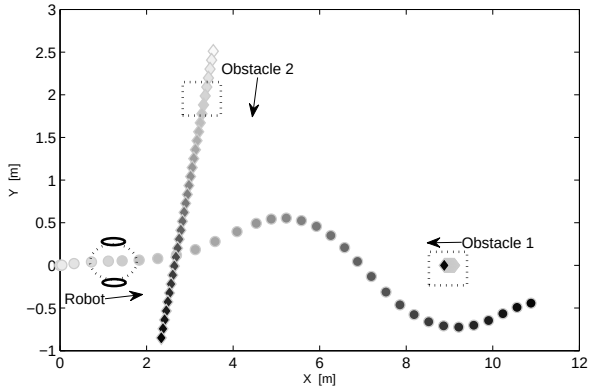

Fig. 13. Trajectory of the robot and 2 moving obstacles

6.4 Procedure

In the experiment, participants were required to manoeuvre a mobile robot, using the haptic control device while they see the video on the screen. The path to be followed by the robot was straight and difficult to follow due to obstacles movements. Figure 12 shows an illustration of the task and the remote environment. The participants were ask to perform the task as quickly as possible, while they faced some visual distractions like checking some signals on a monitor next to the main screen or seeing to other places away the screen.

Before to start the experimentation, a tutorial and training session was provided to each participant in order to get them familiarized with the joystick device and with the procedure.

6.5 Results

Figure 13 shows the trajectory of the robot and obstacles, of one short experiment made. First positions correspond to light points and finals position to darks points. In can be noted that the robot has to change it mains task (following the trajectory straight) in order to avoid collisions.

The collision probability of the robot respect the obstacle 1 and the corresponding visual channel information (P_1

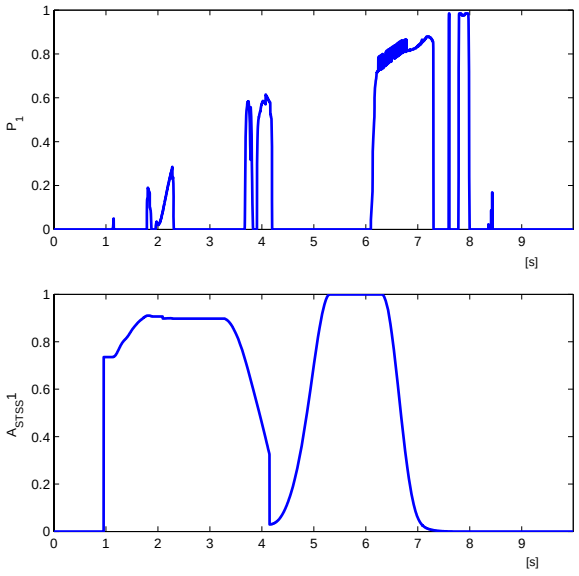

Fig. 14. Experimentation driving the robot across the environment (Robot-Obstacle 1)

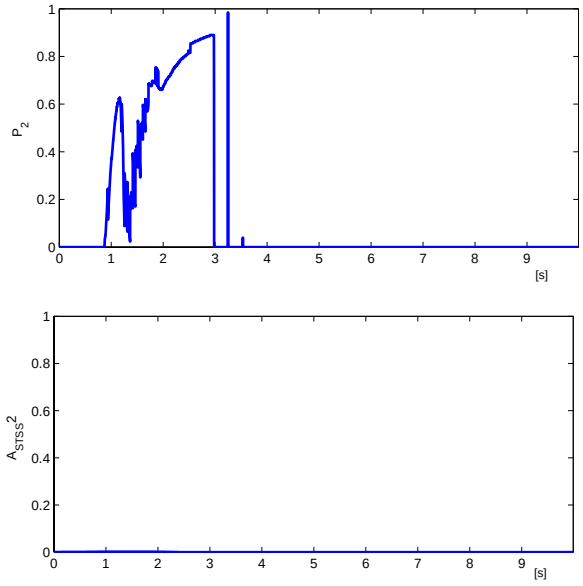

Fig. 15. Experimentation driving the robot across the environment (Robot-Obstacle 2)

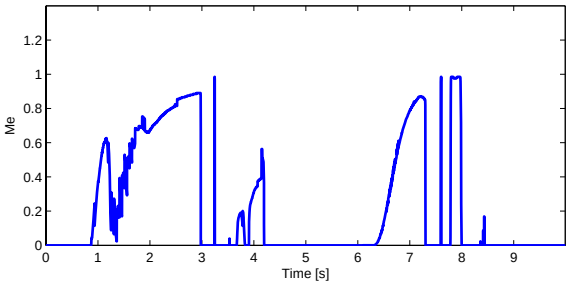

Fig. 16. Experimentation driving the robot across the environment(Metric)

and A_{STSS-1}) are shown in figure 14. On the other hand, figure 15 shows the same information corresponding to the obstacle 2. Finally, figure 16 shows the on-line computation of the visual inattention as it was proposed in this work, conferring direct information about partial aspects of the operator's perception.

At $Time = 0.5s$ or $Time = 5.5s$ (case A), there is not risk around, so despite the human selection of visual attention, the metric has a low value, which means no inattention. At $Time = 2s$ (case B), collision probability of obstacle 1 and 2 are high, and the obstacles are not being captured by his visual channel. Therefore, there is no way to be able to perceive the risk. His inattention is poor (high values of the Me). Finally, at $time = 6.3s$ (case C), collision probability of obstacle 1 is high, but the visual stimulus is present for a deeper perception cognition process, so the inattention is low.

It can be seen that when there exists an obstacle that generates high levels of risk (high collision probability), establishing a situation of risk to the completion of the main task (drive the robot through the desired trajectory), the metric proposed achieve high values if the operator visually ignores such risk (maximum value for 2 objects: $\sqrt{2}$). On the contrary, Me is near to 0 when the human is able to estimates the high collision probability situation based on the cognitive process of his visual channel; or when there is not a collision probability.

7. DISCUSSION

(Lathan and Tracey, 2002) express that teleoperation requires a complex combination of the operator's cognitive, perceptual, and motor skills. So, a human that teleoperates a mobile robots should be helped in order to prevent collisions since the perception of the remote environment is limited. In this sense, force feedback cuing is the option chosen in this work. Our force feedback law include three cuing that helps the user to: (1) keeping low the master tracking error (synchronizing error), (2) reducing the command energy in presence of time delays, and (3) reducing the command energy under visual distractions. The user do not need to identify the specific cue.

An on-line and precise estimation of the perception or attention are difficult to achieve because of the well known *look but do not see*. It is easer to solve a metric upon the non-existent visual information, which lead in poor perception. Non-existent visual information could happen when the human do not look to the source of risk (obstacle with collision probability), or when he has not look at it recently enough. In addition, the way of looking may lead in a degree of visual information available to a deeper cognition process. Fortunately, we want to know when the user is distracted so we can help him with the force feedback. Our metric estimate the visual inattention which leads on poor perception.

The mathematics approach of the method let us to introduce the metric in a control closed loop, and this characteristic is difficult to achieve due to the complex nature of the human factors involved. However, in future works it is needed to improve the model of the variable A, due to the actual one do not considers some important aspects as de distance of the object and its velocity. This will determine the minimum sample time of the visual inspection that is needed to estimate the trajectory of the obstacles.

Poor perception, generally will end on bad commands since perception is the first stage of the situation awareness (SA), and SA comes before a decision making stage. So in order to take advantage on the features of our metric proposed, other important improvement in future works will consist varying the elasticity of the impedance law in the remote robot controller. I can also be proportional to the metric proposed due to a permanent activation can be a bit obtrusive.

Finally, the incorporation of the metric proposed in the force feedback law should be deeply analyzed after defining some evaluation metrics upon the main issues (like high collision probability among the experiment, time to complete the task, heterogeneity on metrics performance, etc.)

8. CONCLUSIONS

In this paper, a definition of a metric on user visual inattention in bilateral teleoperation systems has been proposed. It was also defined and tested a quantitative method for the metric concept proposed, which corresponds to the type of process indices methods and satisfies the requirement to be used as continuous feedback in control applications. This characteristic allows to develop Human-Machine Systems considering the visual selective attention in the design. The method present a theoretical and mathematical framework which allows to incorporate different issues in the processing of visual stimuli, like the one incorporated in this work (fovea region and the short term sensory store). The metric was included in a teleoperation control system, particularly in the local site where the damping of the movement of the master device rise depending on the human visual inattention. The stability of the system is assured and the tuning parameters conditions are given based on a Lyapunov analysis.

Finally, an example of a teleoperation of a mobile robot was considered, where the metric was satisfactorily computed in a human in the loop experiment.

REFERENCES

Andre, A.D., Wickens, C.D., and Moorman, L. (1991). Display formatting techniques for improving situation awareness in the aircraft cockpit. *The International Journal of Aviation Psychology*, 205–218.

Chavez, G.D., Slawinski, E., and Mut, V. (2010). Modeling the inattention of a human driving a car. *Symposium on Analysis, Design, and Evaluation of Human-Machine Systems, IFAC*, 11.

Chen, J., Haas, E., and Barnes, M. (2007). Human performance issues and user interface design for teleoperated robots. *Systems, Man, and Cybernetics, Part C: Applications and Reviews, IEEE Transactions on*, 37(6), 1231–1245. doi:10.1109/TSMCC.2007.905819.

Daly, J. and Wang, D. (2014). Time-delayed output feedback bilateral teleoperation with force estimation for n -dof nonlinear manipulators. *Control Systems Technology, IEEE Transactions on*, 22, 299 – 306.

Diolaiti, N. and Melchiorri, C. (2002). Teleoperation of mobile robot throughhaptic feedback. *in Proc. IEEE Int. Workshop HAVE*, 67–72.

Durso, F.T. and Dattel, A.R. (2004). spam: The real-time assessment of sa, in a cognitive approach to situation awareness: Theory and application. *S. Banbury and S. Tremblay, Eds.*, 137–154.

Durso, F., Hackworth, C., Truitt, T., Crutchfield, J., and Manning, C. (1998). Situation awareness as a predictor of performance in en route air traffic controllers. *Air Traffic Quarterly*, 6, 1–20.

Egeth, H.E. and Yantis, S. (1997). Visual attention: control, representation, and time course. *Annual Review of Psychology*, 48, 268–297.

Elhajj, I., Xi, N., Fung, W.K., Liu, Y.H., Hasegawa, Y., and Fukuda, T. (2003). Supermedia enhanced internet based telerobotics. *Proceedings of the IEEE*, 91, 396–421.

Endsley, M.R. (1995). Measurement of situation awareness in dynamic systems. *Human Factors*, 37, 65–84.

Fiorini, P. and Oboe, R. (1997). Internet-based telerobotics: Problems and approaches.

Fong, T. and Thorpe, C. (2001). Vehicle teleoperation interfaces. *Autonomous Robots*, 11, 9–18.

Hashtrudi-Zaad, K. and Salcudean, S.E. (2001). Analysis of control architectures for teleoperation systems with impedance/admittance master and slave manipulators. *The International Journal of Robotics Research*, 20(6), 419–445.

Hua, C.C. and Liu, X. (2010). Delay-dependent stability criteria of teleoperation systems with asymmetric time-varying delays. *IEEE Trans. Robot.*, 26(5), 925 –932.

Jones, D.G. and Endsley, M.R. (1996). Sources of situation awareness errors in aviation. *Aviation, Space and Environmental Medicine*, 67, 507–512.

Lam, T.M., Boschloo, H.W., Mulder, M., and van Paassen, M.M. (2009). Artificial force field for haptic feedback in uav teleoperation. *IEEE Transactions on Systems, Man, and Cyberneteics-Part A: Systems ans Humans*, 39, 1316–1330.

Lathan, C.E. and Tracey, M. (2002). The effects of operator spatial perception and sensory feedback on human-robot teleoperation performance. *MIT Press Journals*, 11, 368–377.

Luck, S.J. and Hollingworth, A.R. (2008). *Visual Memory*. Oxford University Press, Inc.

McCarley, L. and Wickens, C. (2005). Human factors implications of uavs in the national airpace. *Aviation Human Factor Division, Savoy, IL, Technical Rep.*

Niculescu, S.I. (2001). *Delay Effects on Stability: A Robust Control Approach*. Springer Verlag.

Nuño, E., Ortega, R., Barabanov, N., and Basañez, L. (2008). A globally stable PD controller for bilateral teleoperators. *IEEE Trans. Robot.*, 24(3), 753–758.

Penizzotto, F., Slawiski, E., and Mut, V. (2014). Teleoperation of mobile robots considering human?s commands. In M. Armada, A. Sanfeliu, and M. Ferre (eds.), *ROBOT2013: First Iberian Robotics Conference. Advances in Intelligent Systems and Computing*, volume 253, 601–614. Springer.

Ratwani, R.M., McCurry J., M., and Trafton, J.G. (2010). Single operator, multiple robots: An eye movement based theoretic model of operator situation awareness. *Proceeding of the 5th ACM/IEEE international conference on Human-robot interaction*.

Salmon, P., Stanton, N., Walker, G., and Green, D. (2006). Situation awareness measurement: A review of applicability for c4i environments. *Applied Ergonomics*, 38(1), 225–238.

Sanders, D. (2010). Comparing ability to complete simple tele-operated rescue or maintenance mobile-robot tasks with and without a sensor system. *Sensor Review*, 30, 40 – 50. doi:10.1108/02602281011010781.

Sayers, C. (1999). *Remote control robotics*. Springer-Verlag.

Sheridan, T.B. (1992a). *Telerobotics, Automation, and Human Supervisory Control*. MIT Press Cambridge, MA, USA.

Sheridan, T.B. (1992b). *Telerobotics, Automation and Human Supervisory Control*. MIT Press.

Slawiński, E., Mut, V., Salinas, L., and García, S. (2012). Teleoperation of a mobile robot with time-varying delay and force feedback. *Robotica*, 30(1), 67–77.

Slawiński, E., Mut, V.A., and Postigo, J.F. (2006). Stability of systems with time-varying delay. *Latin American applied research*, 36, 41–48.

Slawiski, E., Mut, V., Salinas, L., and Garca, S. (2012). Teleoperation of a mobile robot with time-varying delay and force feedback. *Robotica*, 30, 67–77. doi:10.1017/S0263574711000427.

Slutski, L. (1998). *Remote manipulation systems: quality evaluation and improvement*. Kluwer Academic Publishers.

Son, H.I., Franchi, A., Chuang, L.L., Kim, J., Blthoff, H.H., and Giordano, P.R. (2013). Human-centered design and evaluation of haptic cueing for teleoperation of multiple mobile robots. *IEEE Transactions on Cybernetics*, 43(2), 597–609.

Taylor, R.M. (1990). Situation awareness rating technique (sart): The development of a tool for aircrew system design. *AGARD Conference Proceedings*, 3–17.

Wickens, C.D. and Hollands, J.G. (2000). *Engineering Psychology and Human Performance - 3 edition*, volume 1. Prentence Hall, New Jersey 07458.

Willaert, B., Reynaerts, D., Van Brussel, H., and Poorten, E. (2014). Bilateral teleoperation: Quantifying the requirements for and restrictions of ideal transparency. *Control Systems Technology, IEEE Transactions on*, 22, 387 – 395.